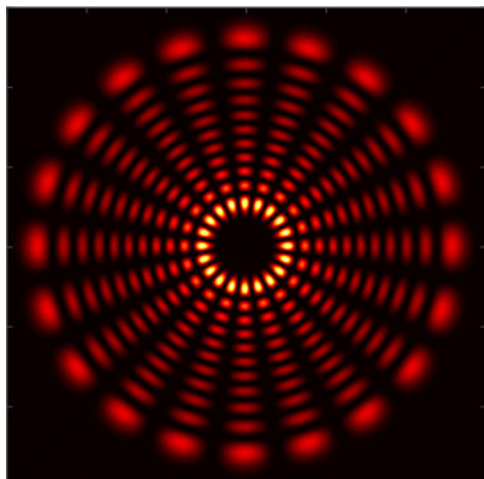


Harnessing Laguerre-Gaussian Beams to Construct Quasi-Nondiffracting Optical Ring Lattices

Volume 10, Number 1, February 2018

Qian Zhao
Lei Gong
Xin-Yao Hu
Pan-Pan Yu
Zi-Qiang Wang
Yin-Mei Li



DOI: 10.1109/JPHOT.2018.2789342
1943-0655 © 2018 IEEE

Harnessing Laguerre-Gaussian Beams to Construct Quasi-Nondiffracting Optical Ring Lattices

Qian Zhao,¹ Lei Gong ,¹ Xin-Yao Hu,¹ Pan-Pan Yu,¹ Zi-Qiang Wang,¹ and Yin-Mei Li^{1,2}

¹Department of Optics and Optical Engineering, University of Science and Technology of China, Hefei 230026, China

²Hefei National Laboratory for Physical Science at the Microscale, Hefei 230026, China

DOI:10.1109/JPHOT.2018.2789342

1943-0655 © 2018 IEEE. Translations and content mining are permitted for academic research only.
Personal use is also permitted, but republication/redistribution requires IEEE permission.
See http://www.ieee.org/publications_standards/publications/rights/index.html for more information.

Manuscript received June 21, 2017; revised December 28, 2017; accepted December 30, 2017. Date of publication January 11, 2018; date of current version January 23, 2018. This work was supported by the National Natural Science Foundation of China under Grant 61535011 and Grant 11374292. Corresponding author: Lei Gong (e-mail: leigong@ustc.edu.cn).

Abstract: We construct a family of optical ring lattices that manifest the quasi-nondiffracting property via superposition of high-radial-order Laguerre-Gaussian beams. A theoretical derivation of the optical ring lattice along with the validity condition is presented, and its evolution behaviors are investigated in comparison with the diffraction-free Bessel beams. Moreover, multiple ultralong bright channels or optical tubes with various transverse profiles can be formed with the ring optical lattices. As a proof of concept, flexible generation of the lattice beams was demonstrated by complex wavefront engineering using a binary digital micromirror device. We anticipate that the quasi-nondiffracting ring lattices and the ultralong optical channels might motivate novel applications in optical trapping and high-resolution microscopy.

Index Terms: Holographic optical components, optical diffraction, optical vortices, optical modulation.

1. Introduction

Laguerre-Gaussian (LG) beams [1] have been widely applied in optical manipulation [2], optical communication [3], nanophotonics [4], and sensing [5] benefiting from their orbital angular momentum (OAM) carrying properties. Meanwhile, the LG superposition modes, including optical ring lattices, Ferris wheels [6] and bottle beams [7], start to draw people's increasing interest. These modes exhibit unique structures, properties and propagation behaviors, enabling applications such as detection of a spinning object [8] or tweezing atoms and Bose condensates (BECs) [9]. Specially, the ring optical lattice [10] is uniquely positioned for studies of ultracold atom trapping where holographic techniques are usually adopted for trap modulation [11]–[13]. In 2007, Arnold *et al.* created a ring optical lattice by two copropagating LG beams with different topological charges, and it was capable of trapping ultracold atoms in red or blue detuned light [6]. From then on, people start to pay attention to the properties of lattice beams and the effect on guiding atoms. For example, S. M. Baumann studied the rotation of the off-axis beam with propagation in free space caused by the Gouy phase [14]. Translation of the intensity profile can be exploited to exert a controllable motion to the trapped atoms. Arnold *et al.* proposed a new method to extend the dark optical trapping

geometries by counter-propagating interference of LG beams [15]. This scheme has been used to produce rotating helical optical tubes or bright channels that can act as an optical atomic conveyor [16]. However, the existing ring lattice beams constructed by the superposition of LG beams are diffracting in nature. It limits the depth of focus of the optical tubes or channels formed, which will deteriorate its performance in accelerating and guiding ultracold atoms.

It is well known that the Bessel beam [17] and the Airy beam [18] are typical diffraction-free beams that also show self-healing property. Interestingly, the self-healing behavior has been observed for the optical ring lattices in the experiment [19]. Naturally, we will ask a question whether the optical ring lattice is able to show some non-diffracting behaviors under a certain physical situation. A recent research [20] reveals that, by imposing the right conditions, the LG beams could propagate quasi-nondiffracting beams like Bessel beams within the same conical volume of existence of Bessel beams. Inspired by this point, we construct a novel kind of ring-shaped optical lattices exhibiting quasi-nondiffracting behaviors by superposition of LG beams with large radial index. In free space, such ring optical lattices are able to create ultralong bright channels or optical tubes that may offer new perspective for optical manipulation of atoms.

By comparing with Bessel beams, the propagation behaviors of the ring optical lattices were investigated via simulation. Furthermore, we experimentally shaped the lattice beams by complex wavefront engineering using a digital micromirror device (DMD) and characterized their propagation behaviors. The three-dimensional structures of the lattice beams were then reconstructed exhibiting ultralong optical tubes or bright channels. Furthermore, we generated various optical channels with different transverse distributions by different combinations of LG modes. These non-diffracting lattice beams with an extended depth of focus may open up new prospective for applications in lattice light-sheet microscopy and moving microscopic objects.

2. Theory

LG modes are solutions of the paraxial diffraction equation, and their complex amplitude under cylindrical coordinates reads [21]

$$U_{LG}(r, \varphi, z) = A_0 \frac{\omega_0}{\omega(z)} \left(\frac{\sqrt{2}r}{\omega(z)} \right)^{|m|} L_n^{|m|} \left(\frac{2r^2}{\omega^2(z)} \right) \exp \left[\frac{-r^2}{\omega^2(z)} - \frac{ikr^2}{2R(z)} + i(2n + |m| + 1)\Phi(z) - im\varphi \right], \quad (1)$$

where

$$\begin{aligned} A_0 &= \frac{1}{\omega_0} \sqrt{\frac{2n!}{\pi(n + |m|)!}}, \quad \Phi(z) = \arctan \left(\frac{z}{L_D} \right), \quad \omega(z) = \omega_0 \sqrt{1 + \left(\frac{z}{L_D} \right)^2}, \\ L_D &= \frac{\pi\omega_0^2}{\lambda}, \quad \text{and} \quad R(z) = z \left[1 + (L_D/z)^2 \right]. \end{aligned} \quad (2)$$

A_0 is the amplitude, ω_0 is the beam waist at $z = 0$, k is the wavenumber, and L_D is the Rayleigh range of the Gaussian envelope. $L_n^{|m|}$ is the associated Laguerre polynomial with n and m as the radial and azimuthal indices, respectively.

In general, the LG beams share the similar diffraction behavior with the Gaussian beam due to their Gaussian envelope indicated by Eq. (2). However, sometimes they show a different behavior, and it depends on the physical situation. For instance, if the radial index $n \gg 1$, the complex field of LG beams at $z = 0$ plane can be deduced as [20]

$$U_{LG}(r, \varphi) \approx A_0 \frac{\Gamma(n + |m| + 1)}{n!N^{|m|/2}} J_m \left(2\sqrt{2N} \frac{r}{\omega_0} \right) \times \exp(-im\varphi) \quad (3)$$

where A_0 is the amplitude, $J_m(\cdot)$ is the m -th Bessel function of the first-kind, and $\Gamma(\cdot)$ is the gamma function. The equation indicates that such a LG beam has a similar profile with the Bessel beam having the same topological charge. Thus, we have the relation of the radial frequency $k_t = 2\sqrt{2N}/\omega_0$, where $N = n + (|m| + 1)/2$.

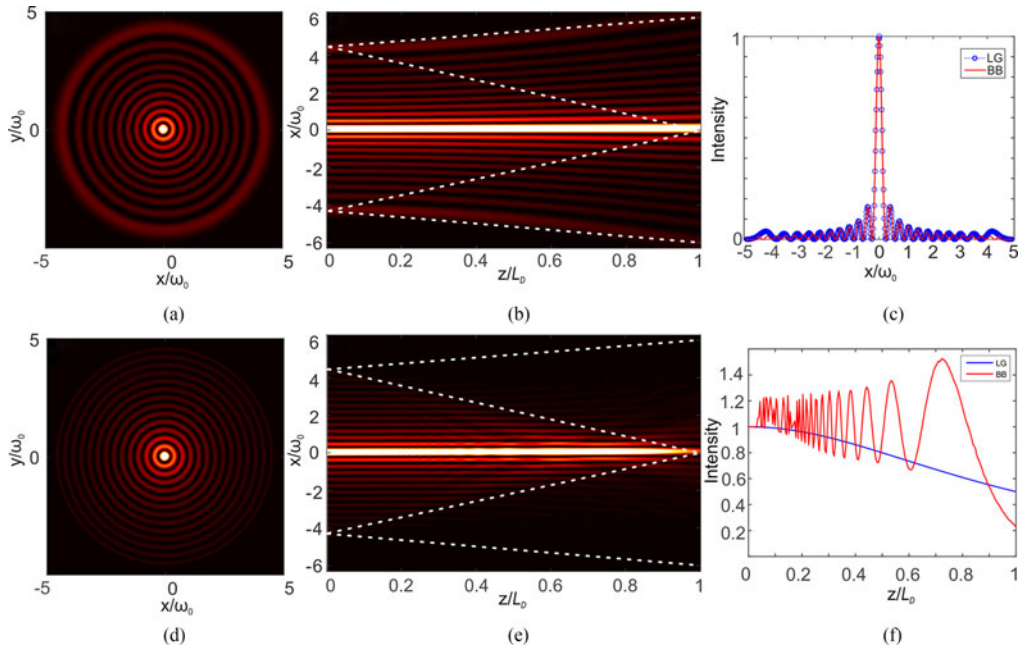


Fig. 1. The quasi-nondiffracting property of a LG beam. (a) and (c) The transverse distribution of a $L G_{10}^0$ beam and the truncated Bessel beam, respectively. (b) and (d) The beam evolution of LG beam and Bessel beam on the xz plane. (e) The comparison of the one-dimensional transverse profiles of the LG beam and the Bessel beam. (f) The comparison of on-axis intensity of the LG beam and the truncated Bessel beam.

Theoretically, the range of an ideal Bessel beam tends to be infinite. Whereas, the rings in a high-radial-order LG Beam with pair indices m and n are confined within a disk with a radius of $R = \omega_0\sqrt{2N}$ [22]. Here, we use this radius to truncate the transverse distribution of the Bessel beam, and compare the propagation behavior of LG beams within the same conical volume of existence of Bessel beams. Since the Bessel beam can be considered as a set of waves propagating on a cone with angle of θ , the maximum non-diffraction distance of the truncated Bessel beam can be calculated with $Z_{\max} = R/\tan\theta \approx R/(k_t/k) \equiv L_D$. This relation shows that the maximum propagation distance of a Bessel Beam is practically identical to the diffraction length of a LG Beam under the similar circumstances. Note that the distance L_D defines the space within which the LG Beam can be considered quasi-nondiffracting, resembling the Bessel beam [20].

As an example, we first numerically studied the propagation behavior of a $L G_{10}^0$ beam [Fig. 1(a)] in comparison with the zero-order Bessel beam [Fig. 1(c)] truncated by a disk of radius $R = \sqrt{21}\omega_0$. The results are shown in Fig. 1. The transverse and longitudinal coordinates are normalized to ω_0 and L_D , respectively. At $z = 0$ plane, the transverse intensity profiles of two beams coincide very well especially in the central part of the disk with a radius of $2\omega_0$ containing the first $n/2$ rings. It can be verified via the x -axis intensity profiles, as shown in Fig. 1(e). In addition, the $x - z$ intensity distributions of two beams were calculated and are presented in Figs. 1(b) and 1(d). We marked the triangular region of the existence of Bessel beam as well as the external hyperbola of the LG beam with white dashed lines. It can be observed that the LG beam shares almost the same conical region of existence with the truncated Bessel beams. Then the on-axis intensity distribution was analyzed, and is presented in Fig. 1(f). It can be seen that the normalized intensity of Bessel beam at $z = L_D$ decays to less than 0.25, while that of LG beam decays to about 0.5. At the region of $z < 0.9L_D$, the intensity of the LG beam is comparable to that of Bessel beam. Therefore, the LG beams with a large radial index are found to resemble the Bessel beams, manifesting the behavior of quasi-nondiffracting.

Inspired by this point, here we construct a new kind of ring-shaped optical lattices exhibiting quasi-nondiffracting property by superposition of high-radial-order LG beams. It has been

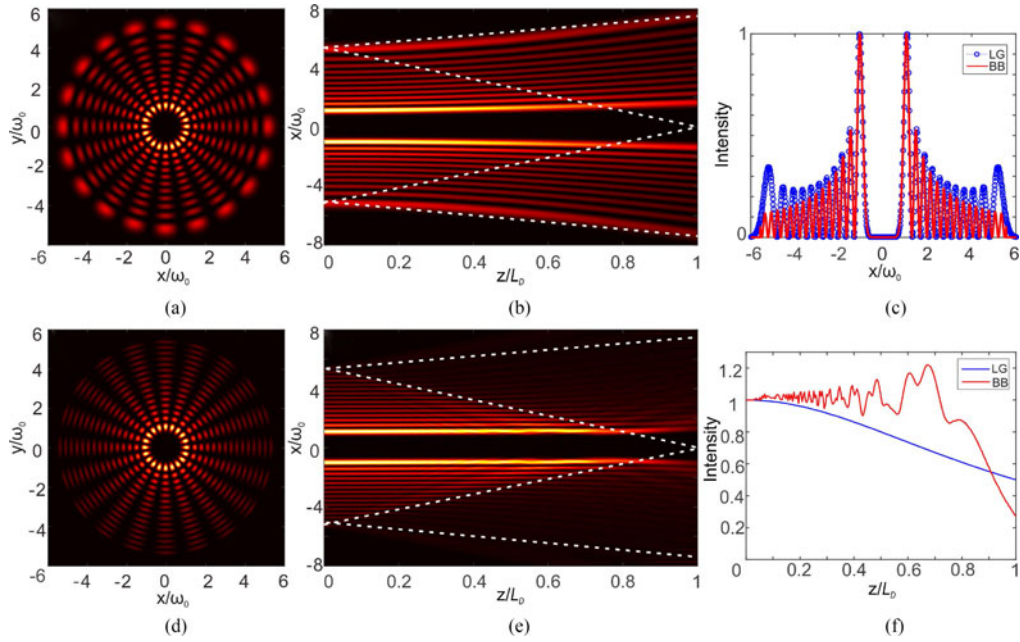


Fig. 2. The ring optical lattices constructed by LG beams and Bessel beams. (a) and (b) The transverse distribution of the ring lattices superposed by two LG modes ($L G_{10}^{10}$, $L G_{10}^{-10}$) and two truncated Bessel modes with indexes ($m = 10, -10$). (b) and (d) The corresponding x - z intensity profiles of the two ring lattices. (e) The comparison of the transverse profiles of the two ring lattices at the $y = 0$ plane. (f) The comparison of maximum intensity versus propagation distance of the two ring lattices.

demonstrated that any diffraction-free beam can be formed with a linear combination of the Bessel modes having the same transverse wavenumber. Likewise, in order to construct the diffraction-free ring lattice beams, the parameter $k_l = 2\sqrt{2N}/\omega_0$ in Eq. (3) should be identical for all the component LG beams. In other words, only if the values of $N = n + (|m| + 1)/2$ are the same, the combined beam exhibits quasi-nondiffracting property. Therefore, we can construct optical ring lattices with various transverse profiles via selection of different combinations of $L G_n^m$, which offer one more degree of freedom, i.e., radial index, for structure modulation than Bessel beams.

For instance, two ring lattice beams are constructed by superposition of two LG modes ($L G_{10}^{10}$, $L G_{10}^{-10}$) and two truncated Bessel modes with indexes $m_1 = 10, m_2 = -10$, respectively. Their ring-lattice profiles are presented in Figs. 2(a) and 2(c), containing $2|m|$ intensity petals along the azimuthal direction [19]. As demonstrated in Fig. 2(e), the superposition modes have the similar intensity distribution within the central part, just like the individual mode's performance. The propagation of the central ring lattice along z -axis forms multiple bright channels with extended depth of focus. The length of the ultralong optical channels formed by superposition LG modes is comparable to that of Bessel beams, whose central triangular regions of quasi-nondiffracting (dashed lines) are shown in Figs. 2(b) and 2(d). In addition, their normalized intensity distributions of the bright channels along z -axis were compared and are shown in Fig. 2(f). We note that from $z = 0$ plane to $z = L_D$ plane, the intensity of the optical channel constructed by LG beams decays to about 0.5, while the intensity of the bright channel created by truncated Bessel beams decays to less than 0.3. The findings show that we can construct quasi-nondiffracting ring optical lattices with LG beams, and ultralong bright channels can be formed with such ring optical lattices that are distinguished from the previously reported ones.

3. Experiment

As a proof of concept, the flexible generation of the ring lattice beams were demonstrated by complex wavefront engineering using a binary DMD. A programmable DMD is able to switch at rates up to 32 kHz, enabling dynamic wavefront shaping and various applications in beam optics [23]–[25].

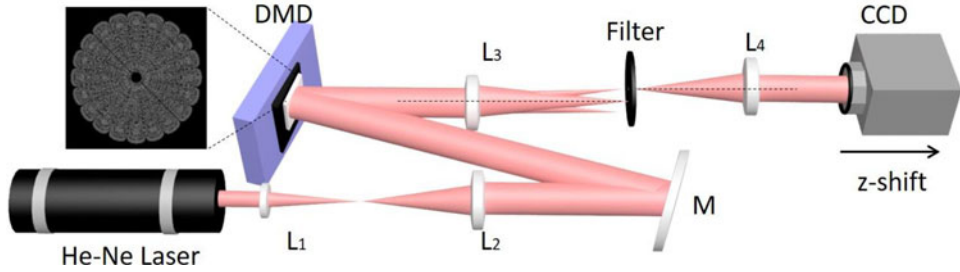


Fig. 3. Experimental setup. The inset: A typical binary hologram designed by the super-pixel method. L, lens; M, mirror; CCD camera, charge-coupled device camera.

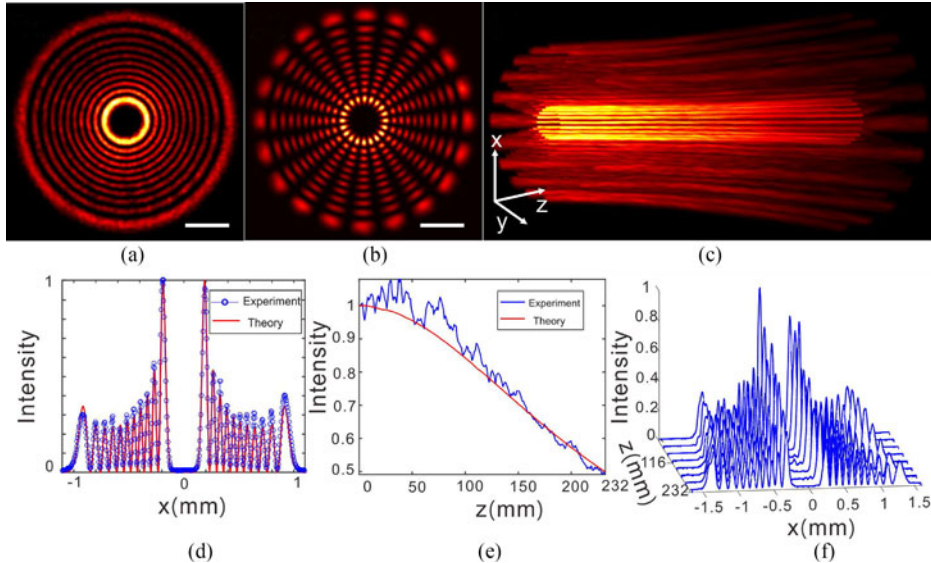


Fig. 4. Experimental generation of the ring optical lattice. The transverse intensity distribution of (a) the LG_{10}^{10} beam and (b) the ring optical lattice superposed by two LG modes ($LG_{10}^{10}, LG_{-10}^{-10}$). (c) The 3D view of spatial evolution of the ring optical lattice. (d) The 1D intensity distribution of the ring optical lattice. The blue and red lines represent the experimental and theoretical curves, respectively. (e) The measured (blue line) and theoretical (red line) maximum intensity of the bright channel versus the propagation distance. (f) The 3D plot of the field evolution. The scale bar is 0.5 mm.

Here we adopt a super-pixel method to fully engineer the spatial amplitude and phase of an incident beam using a binary DMD (1920×1080 pixels resolution, ALP 4395, Vialux) combined with a low pass filter [26], [27]. The experimental setup is sketched in Fig. 3. A laser beam ($\lambda = 632.8$ nm) was expanded by a telescope (L_1 and L_2) and steered to fully illuminate the surface of the DMD. Then, a binary amplitude hologram (the inset) designed by the super-pixel method was projected onto the DMD to shape the desired field. A 4f configuration consisted by L_3 ($f_3 = 300$ mm) and L_4 ($f_4 = 100$ mm) and a low pass filter were used to select the first-diffraction-order beam. Then we could obtain the desired field at the image plane and observe the field evolution along the propagation direction with a moveable CCD camera (D752, PixeLINK).

A quasi-nondiffracting LG_{10}^{10} beam and the corresponding ring lattice superposed by two LG modes ($LG_{10}^{10}, LG_{-10}^{-10}$) were generated with the DMD. Their cross-sectional images recorded at the image plane are illustrated in Figs. 4(a) and 4(b). The radius of the central bright ring of the two beams are the same because of their same order of azimuthal phase. Then, the 1D intensity profile of the lattice beam was reconstructed at the plane of $y = 0$. The experimental result [blue line in Fig. 4(d)] is well verified via the comparison with theoretical distribution (red line). Further, we investigated the spatial evolution of the beam by collecting a series of cross-sectional images

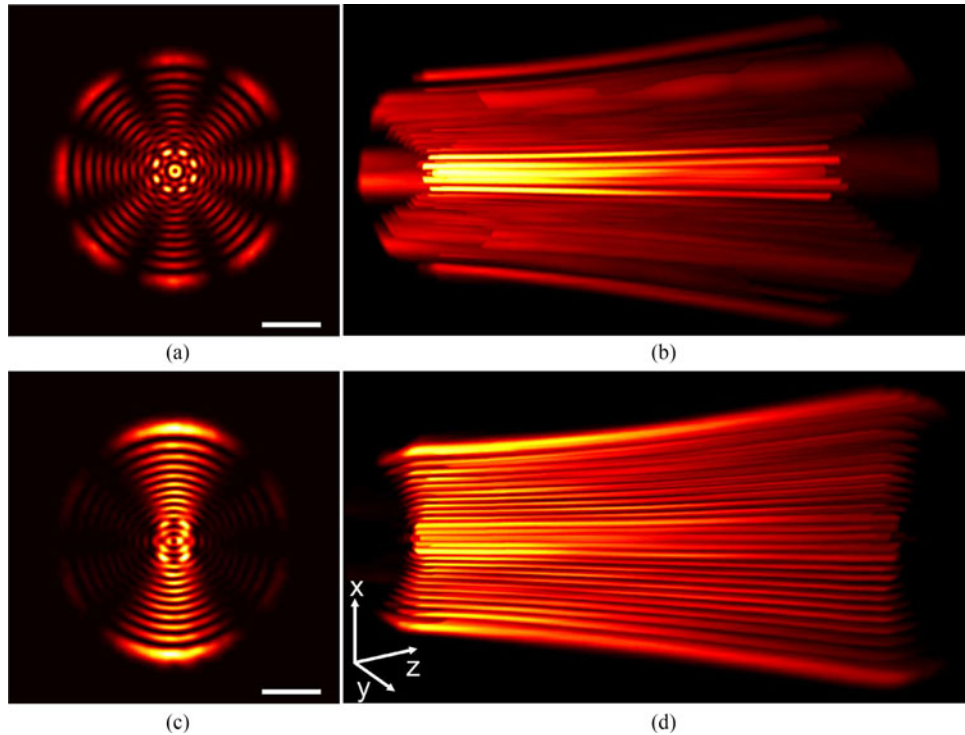


Fig. 5. Generation of ring optical lattices with different transverse profiles. (a) The transverse profile of the lattice beam constructed by superposition of $L G_{12}^1$ and $L G_9^{-7}$. (b) The 3-D view of the ultralong optical tube. (c) The transverse profile of the lattice beam constructed by four LG modes ($L G_{10}^5$, $L G_{11}^3$, $L G_{12}^1$, $L G_9^7$) and (d) the reconstructed spatial structure. The scale bar is 0.5 mm. The propagation distance is set to be the Rayleigh length of 232 mm.

along the light propagation direction ($L_D = 232$ mm in the experiment). Based on the recorded images, the x-z intensity distribution [Fig. 4(f)] for the generated lattice beam was reconstructed, from which the normalized intensity of bright channels (blue line) versus propagation distance was calculated, as illustrated in Fig. 4(e) together with the theoretical one (red line). According to the theory above, the results show that a quasi-nondiffracting beam with a ring lattice profile was generated. In addition, the 3D view of the optical field derived from the stack of images is also presented in Fig. 4(c), which manifests the ring lattice beam is able to naturally create ultralong bright channels over propagation. The structure of lattice beam within the central region is found to be stable along with propagation, and this is a direct indication of its quasi-nondiffracting behaviors.

Here in above, it has been demonstrated that ring-shaped bright channels can be constructed by superposition of LG beams with opposite topological charges. Whereas, ultralong optical tube can also be created with quasi-nondiffracting LG beams, as illustrated in Fig. 5(b). Such a ring lattice beam is constructed by the superposition of two modes of $L G_{12}^1$ and $L G_9^{-7}$. Its transverse profile is shown in Fig. 5(a), exhibiting a petal-like structure with a single ring in the center. Furthermore, ring lattice beams with various transverse profiles can be constructed. It benefits from the fact that LG mode has two independent parameters (n, m) that decide its field distribution. Thus, we can design the transverse profiles of lattice beams by choosing arbitrary combination only if the individual parameter pairs satisfy the same N which equals to $n + (|m| + 1)/2$. As an example, in Figs. 5(c) and 5(d), we show a quasi-nondiffracting beam with transverse profile of an ‘hourglass’ by superimposing four modes of $L G_{10}^5$, $L G_{11}^3$, $L G_{12}^1$, and $L G_9^7$. Note that the DMD is capable of fast switching among various ring lattice beams, which may benefit dynamic application scenes such as imparting a global motion to the trapped atoms. Thus, our method provides high flexibility in the generation of ring-shaped optical lattices.

4. Conclusion

In summary, we have exploited the unique properties of high-radial-order Laguerre-Gaussian (LG) beams to construct optical ring lattices that manifest diffraction-free behaviors. The quasi-nondiffracting lattice beams are able to form multiple optical channels or tubes naturally with extended depth of focus. Their evolution behaviors were studied by comparison with Bessel beams. To verify the theoretical predictions, a flexible DMD-based scheme was employed to generate the ring optical lattices with different transverse distributions. Furthermore, ultralong optical channels and tubes were reconstructed experimentally. Our work brings new perspective for LG beams, and the generated optical ring lattice with distinct propagation property may find potential applications in optical trapping or high-resolution microscopy.

References

- [1] L. Allen, M. W. Beijersbergen, R. Spreeuw, and J. Woerdman, "Orbital angular momentum of light and the transformation of Laguerre-Gaussian laser modes," *Phys. Rev. A*, vol. 45, no. 11, 1992, Art. no. 8185.
- [2] M. Padgett and R. Bowman, "Tweezers with a twist," *Nature Photon.*, vol. 5, no. 6, pp. 343–348, 2011.
- [3] G. Gibson *et al.*, "Free-space information transfer using light beams carrying orbital angular momentum," *Opt. Exp.*, vol. 12, no. 22, pp. 5448–5456, 2004.
- [4] M. Dienerowitz, M. Mazilu, P. J. Reece, T. F. Krauss, and K. Dholakia, "Optical vortex trap for resonant confinement of metal nanoparticles," *Opt. Exp.*, vol. 16, no. 7, pp. 4991–4999, 2008.
- [5] A. Belmonte, C. Rosales-Guzmán, and J. P. Torres, "Measurement of flow vorticity with helical beams of light," *Optica*, vol. 2, no. 11, pp. 1002–1005, 2015.
- [6] S. Franke-Arnold *et al.*, "Optical ferris wheel for ultracold atoms," *Opt. Exp.*, vol. 15, no. 14, pp. 8619–8625, 2007.
- [7] J. Arlt and M. Padgett, "Generation of a beam with a dark focus surrounded by regions of higher intensity: The optical bottle beam," *Opt. Lett.*, vol. 25, no. 4, pp. 191–193, 2000.
- [8] M. P. J. Lavery, F. C. Speirsits, S. M. Barnett, and M. J. Padgett, "Detection of a spinning object using light's orbital angular momentum," *Science*, vol. 341, no. 6145, pp. 537–540, 2013.
- [9] R. Campbell and G.-L. Oppo, "Stationary and traveling solitons via local dissipation in Bose-Einstein condensates in ring optical lattices," *Phys. Rev. A*, vol. 94, no. 4, 2016, Art. no. 043626.
- [10] N. Houston, E. Riis, and A. Arnold, "Reproducible dynamic dark ring lattices for ultracold atoms," *J. Phys. B: Atomic, Mol. Opt. Phys.*, vol. 41, no. 21, 2008, Art. no. 211001.
- [11] A. L. Gaunt and Z. Hadzibabic, "Robust digital holography for ultracold atom trapping," *Sci. Rep.*, vol. 2, 2012, Art. no. 721.
- [12] F. Buchieri *et al.*, "Holographic optical traps for atom-based topological Kondo devices," *New J. Phys.*, vol. 18, no. 7, 2016, Art. no. 075012.
- [13] D. Bowman, P. Ireland, G. D. Bruce, and D. Cassetta, "Multi-wavelength holography with a single spatial light modulator for ultracold atom experiments," *Opt. Exp.*, vol. 23, no. 7, pp. 8365–8372, 2015.
- [14] S. Baumann, D. Kalb, L. MacMillan, and E. Galvez, "Propagation dynamics of optical vortices due to Gouy phase," *Opt. Exp.*, vol. 17, no. 12, pp. 9818–9827, 2009.
- [15] A. S. Arnold, "Extending dark optical trapping geometries," *Opt. Lett.*, vol. 37, no. 13, pp. 2505–2507, 2012.
- [16] A. Al Rashed, A. Lytras, V. E. Lembessis, and O. M. Aldossary, "Guiding of atoms in helical optical potential structures," *J. Phys. B: Atomic, Mol. Opt. Phys.*, vol. 49, no. 12, 2016, Art. no. 125002.
- [17] D. McGloin and K. Dholakia, "Bessel beams: Diffraction in a new light," *Contemp. Phys.*, vol. 46, no. 1, pp. 15–28, 2005.
- [18] G. Siviloglou, J. Broky, A. Dogariu, and D. Christodoulides, "Observation of accelerating Airy beams," *Phys. Rev. Lett.*, vol. 99, no. 21, 2007, Art. no. 213901.
- [19] P. Vaity and R. Singh, "Self-healing property of optical ring lattice," *Opt. Lett.*, vol. 36, no. 15, pp. 2994–2996, 2011.
- [20] J. Mendoza-Hernandez, M. L. Arroyo-Carrasco, M. D. Iturbe-Castillo, and S. Chavez-Cerda, "Laguerre-gauss beams versus bessel beams showdown: Peer comparison," *Opt. Lett.*, vol. 40, no. 16, pp. 3739–3742, 2015.
- [21] A. E. Siegman, *Lasers*, vol. 37. Mill Valley, CA, USA: Univ. Sci. Books, pp. 462–466, 1986.
- [22] R. L. Phillips and L. C. Andrews, "Spot size and divergence for Laguerre Gaussian beams of any order," *Appl. Opt.*, vol. 22, no. 5, pp. 643–644, 1983.
- [23] Z.-X. Fang, Y.-X. Ren, L. Gong, P. Vaveliuk, Y. Chen, and R.-D. Lu, "Shaping symmetric Airy beam through binary amplitude modulation for ultralong needle focus," *J. Appl. Phys.*, vol. 118, no. 20, 2015, Art. no. 203102.
- [24] D. Wang, E. H. Zhou, J. Brake, H. Ruan, M. Jang, and C. Yang, "Focusing through dynamic tissue with millisecond digital optical phase conjugation," *Optica*, vol. 2, no. 8, pp. 728–735, 2015.
- [25] X. Zhang and P. Kner, "Binary wavefront optimization using a genetic algorithm," *J. Opt.*, vol. 16, no. 12, 2014, Art. no. 125704.
- [26] L. Gong *et al.*, "Observation of the asymmetric Bessel beams with arbitrary orientation using a digital micromirror device," *Opt. Exp.*, vol. 22, no. 22, pp. 26763–26776, 2014.
- [27] Q. Zhao, L. Gong, and Y.-M. Li, "Shaping diffraction-free Lommel beams with digital binary amplitude masks," *Appl. Opt.*, vol. 54, no. 25, pp. 7553–7558, 2015.